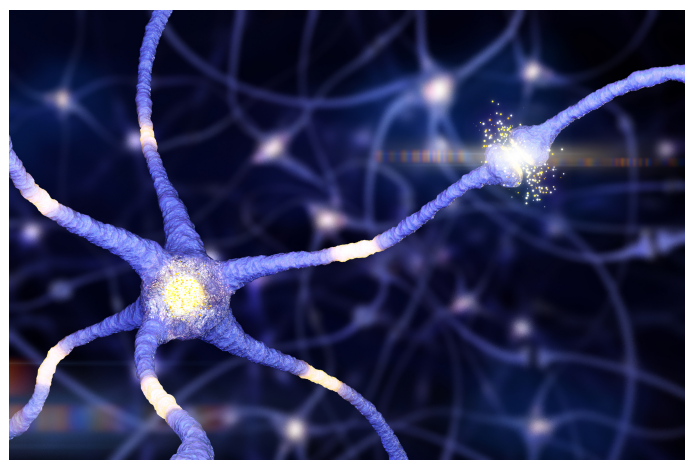


UNIVERSITÉ DE LIÈGE

SYST0017-1 ADVANCED TOPICS IN SYSTEMS AND CONTROL

Pattern formation in intracortical neuronal fields



BOXUS FLORENT S201766
CASARIL MAUD S202160

TEACHERS : P. DAUBY
G. DRION
Teaching assistant : A. FYON

Academic year : 2023-2024

1 Goal of the project

The goal of this project is to understand and modelize the formation of patterns in intracortical neuronal fields. To do so, the paper [Pattern formation in intracortical neuronal fields](#) written by Axel Hutt, Michael Bestehorn and Thomas Wennekers is used. This paper explains a model for both excitatory and inhibitory connections between intercortical neurons. Many studies have already been conducted to build models with both single coupled neurons and continuous neuronal fields. The specificity of the model built in the paper is that the delay for short-range continuous fields is taken into account. Because such model has already been studied but for long range condition, the authors have extended the model to shorter range. Based on this derived model, several configurations will be tested to highlight the various patterns which can appear. We will put the emphasis on the mechanism of formation of the formation of self organized states.

2 Derived model

2.1 Biological behaviour

It is known that in specific cortical layers, neurons are aligned in a particular manner to produce extensive overall activity meaning that neurons interact with other neurons. These interactions can be excitatory or inhibitory by Dale's principle. This principle state that a neuron performs the same chemical action over all its synapses, regardless of which neuron it is connected to. It also seems logical that neurons will be mainly affected by close neighbors rather than distant ones which is linked to the fact that there is a delay in the transmission of the action potential between neurons. Connections between neurons are myelinated axonal fibres which enables to increase the velocity of the information but in intracortical area, the velocity is slow so the delay is big. In the present problem, the derived model must highlight the creation of patterns due to the behavior of neurons which are close to each other taking into account delay due to the distance between each neuron. We will consider both excitatory and inhibitory short-range are un-myelinated.

In the present model, one considers pyramidal neurons. Such neurons can generate pulses, those pulse travel along the axis and arrive at the synapses. When an action potential reaches a chemical synapse, voltage dependent Ca^{2+} open, causing Ca^{2+} to flow in and the synapse releases then neurotransmitters. These neurotransmitters then cause the post synaptic neuron dendrite to conduct another action potential to the soma, where it sums up with other's action potential. This complex mechanism allows considering both inhibitory and excitatory phenomenon. The delay is mainly caused by this post-synaptic action potential by dendrites.

2.2 Derivation of equations

Due to experiences, it appears that the membrane potential V of a pyramidal neuron can be linked with the pulse rate P by a sigmoid function, as it is commonly accorded in the neuroscience field. According to this, the pulse rate in a continuous neuronal field is given by :

$$P(x, t) = S_{max}S[V(x, t)] = \frac{S_{max}}{1 + e^{-c(V(x, t) - V_r)}} \quad (1)$$

where S is the sigmoid function, S_{max} is the maximum pulse rate, c is a parameter that determines the steepness of the sigmoid function and V_r represents the mean threshold. The Eq. 1 is valid under the hypothesis that all neurons are identical. But, regarding the goal of the project, it is necessary to distinguish inhibitory and excitatory neurons. To do so, an

expression for the pulse rate can be derived for both the entering pulse rate in excitatory (e) and inhibitory (i) synapses

$$\overline{P_{e,i}}(x, t) = \int_{\Gamma} dx' \beta_{e,i} f_{e,i}(x, x') P(x', t - \frac{|x - x'|}{v_{e,i}}) + \mu_{e,i} P^{ext}(x, t). \quad (2)$$

The distinction can be made due to the introduction of the synaptic connection probability distributions $f_{e,i}$ and the weight factors $\beta_{e,i}$. Intuitively, the first term of the Eq. 2 represents the sum over the contribution of all neurons (inhibitory or excitatory) taking into account the distance between the impacted neuron located in x and the perturbing neuron located in x' (the distance being represented by the probability density function f). The delay is computed according to the definition of a linear motion using the finite velocity $v_{e,i}$ and appears in the equation subtracted from physical time. In practice, this means that the pulse rate at time t is influenced by the pulse rate of the neuron located at x' at time t' , the time t' being smaller if the distance is bigger. A second term is also there and represents an external pulse activity P^{ext} multiplied by the coupling parameter $\mu_{e,i}$.

The relationship between incoming activity and postsynaptic excitatory (e) and inhibitory (i) potentials is given as $V_{e,i}(x, t)$. Now we have an equation describing the pulse rate, one should want to describe the time behavior of the synapse. A relation modeling the post-synaptic potential have to be found. The synaptic response to incoming activity is obtained with a convolution between the impulse response $h_{e,i}(t)$ (modeling time dependency pf the synapse with respect to the pulse rate) and the postsynaptic potentials, which gives :

$$V_{e,i}(x, t) = g_{e,i} \int_{-\infty}^t d\tau h_{e,i}(t - \tau) \overline{P_{e,i}}(x, \tau). \quad (3)$$

Please note that this procedure is valid if the system is linear time invariant. In the Eq. 3, $g_{e,i}$ stands for the synaptic gain factors for both excitatory and inhibitory case. Regarding this two definitions, the membrane potential can be written as : $V = V_e - V_i$. Indeed, this allows to combine both excitatory and inhibitory synapse effects. In addition, some assumptions can be made to simplify the problem :

1. after an identical pulse, the impulse response functions of excitatory and inhibitory synapses are the same so $h_e = h_i = h$ and the sigmoid function is also the same for both cases so $S_e = S_i = S$,
2. only intracortical connections are taking into account and the connections are made with a common propagation velocity $v_e = v_i = v$ on an un-myelinated axonal fibers,
3. the external pulse activity P^{ext} is excitatory so $\mu_i = 0$ and it leads to $g_e \mu_e = \mu$,
4. synaptic connections are only isotropic (same properties in all directions) and homogeneous (same in the whole space).
5. $a_{e,i} = g_{e,i} * \beta_{e,i}$ is a parameter gathering the weight factors and the synaptic gains.

Let us inject the equation 2 in the equation 3 and use the mentioned assumptions, one gets the expression for the membrane potential :

$$V = V_e - V_i = \int_{-\infty}^t d\tau h(t - \tau) \left[\int_{\Gamma} dx' a_e f_e(x, x') S \left[V(x', \tau - \frac{|x - x'|}{v}) \right] + \mu P(x, \tau) \right] \quad (4)$$

$$- \int_{-\infty}^t d\tau h(t - \tau) \left[\int_{\Gamma} dx' a_i f_i(x, x') S \left[V(x', \tau - \frac{|x - x'|}{v}) \right] \right] \quad (5)$$

$$= \int_{-\infty}^t \int_{\Gamma} dx' h(t - \tau) \times \left[(a_e f_e(x, x') - a_i f_i(x, x')) S \left[V(x', \tau - \frac{|x - x'|}{v}) \right] + \mu P(x, \tau) \right] \quad (6)$$

In the above expression, the impulse response is still unknown. Detailed studies about synapses' mechanisms indicates that it can be expressed as

$$h(t) = \frac{\alpha_1 * \alpha_2}{\alpha_1 - \alpha_2} * (\exp[-\alpha_1 t] - \exp[-\alpha_2 t]) \quad (7)$$

with both parameters $\alpha_1, \alpha_2 > 0$.

From the theoretical course, it is known that this is can be considered a Green function of the second order linear operator :

$$\hat{L} = \left(\frac{\partial}{\partial t} + \alpha_1 \right) * \left(\frac{\partial}{\partial t} + \alpha_2 \right) \quad (8)$$

with $\hat{L}h(t) = \delta(t)$ by definition of Green's functions

For the synaptic connectivity functions, the model assumes exponential decay as the neurons are further away from each others. So

$$f_{e,i}(x) = \frac{1}{2r_{e,i}} * \exp\left[-\frac{|x - x'|}{r_{e,i}}\right] \quad (9)$$

Now, the linear operator \hat{L} can be applied on Eq. 6, using the result 2.2 and knowing $\int_{-\infty}^t \delta(+\infty) = 1$:

$$\hat{L}V(x, t) = \left[\frac{\partial^2}{\partial t^2} + \left(\alpha + \frac{1}{\alpha} \right) + 1 \right] V(x, t) \quad (10)$$

$$= \frac{1}{2} \int_{\Gamma} dx' (a_e e^{-(|x-x'|)} - a_i r e^{-(|x-x'|)r}) \times S\left[V(x', t - \frac{|x - x'|}{v})\right] + \mu P(x, t) \quad (11)$$

after the following adimensionalization $t \rightarrow t\sqrt{\alpha_1\alpha_2}$, $x \rightarrow \frac{x}{r_e}$, $v \rightarrow \frac{v}{r_e}\sqrt{\alpha_1\alpha_2}$. One also defines $\alpha = \sqrt{\frac{\alpha_1}{\alpha_2}}$ for timescale and $r = \frac{r_e}{r_i}$ as the ration of connection parameters.

The synaptic connectivity function which appears in the above equation can be defined as :

$$K(|x - x'|) = a_e * \exp[-|x - x'|] - a_i r \exp[-|x - x'|r] \quad (12)$$

which is graphically represented on Fig. 1. On this plot, one can see that if $r < 1$, the synaptic connections take large positive values for small distances and small negative values for larger distance. This is a case of local excitation and lateral inhibition type. Indeed, if one checks the equation 11, this value of K is integrated over all the neighboring neurons, so the negative value (for inhibition effects) will decrease the membrane potential, making it less likely to spike while positive values of K increase the membrane potential, making it more prone to spiking. On the opposite case, the result can be seen on Fig. 1. Indeed, for $r < 1$, a local inhibition lateral excitation type can be seen. But taking a look at the values on the plot shows that the local inhibition is much stronger than local excitation because values of inhibition are much higher. This has been proven by other studies.

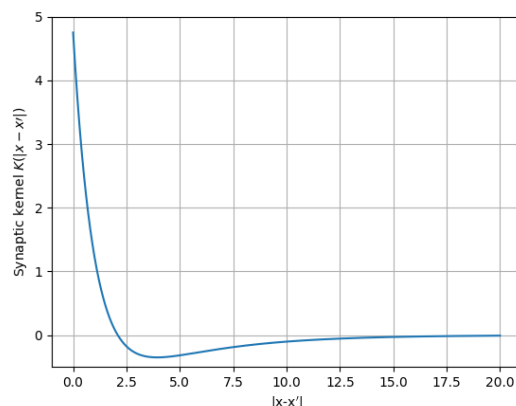
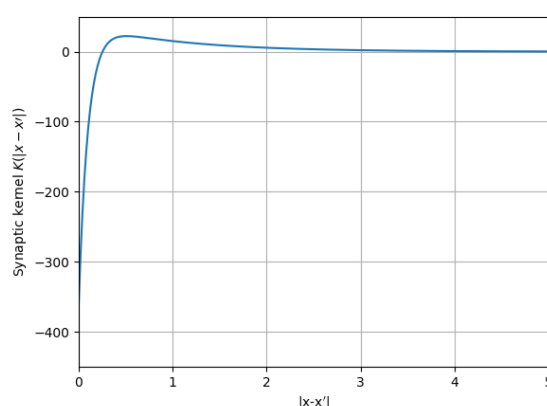
(a) Synaptic connections for $r=0.25$, $a_e=6$, $a_i=5$ (b) Synaptic connections for $r=10$, $a_e=41$, $a_i=40$

FIGURE 1 – Synaptic connections

2.3 Stability of a homogeneous rest state

For many biological systems, we can observe self-organized patterns in systems when those are pushed out of stability by a perturbation (figure 2).

In order to study those formations, a stationary (time independent) homogeneous external excitation is applied (remember that an external inhibition is not applied) :

$$P(x, t) = P_0 \quad (13)$$

and a periodic spatial field is considered.

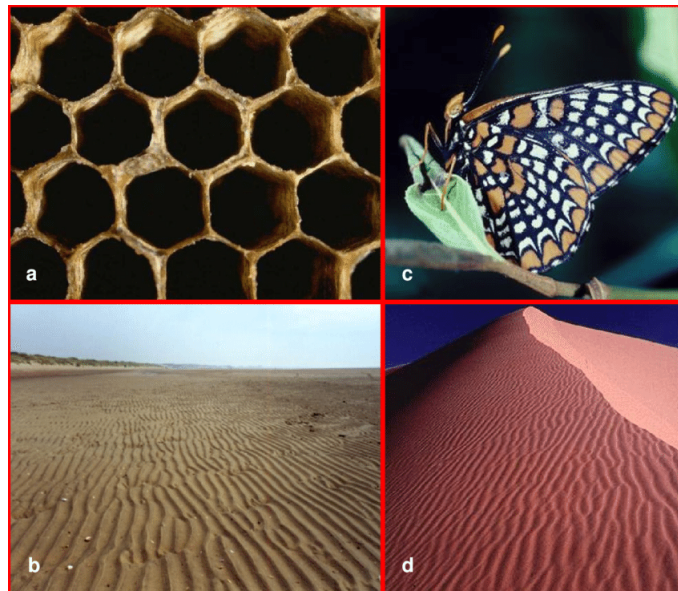
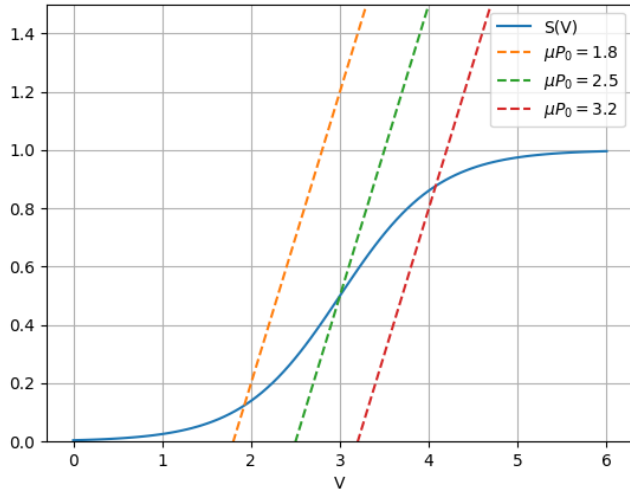


FIGURE 2 – Some self organized patterns in nature

Regarding the equation 11, at the resting state, there is no more time dependence so the time derivatives equal to 0. By moving the left-hand side V_0 (the only term not derived with respect to time) to the right hand, the transcendent equation can be written as :

$$f(V_0) = (a_e - a_i)S(V_0) - V_0 + \mu P_0. \quad (14)$$

The solution for the rest voltage is obtained by solving $f(V_0) = 0$. This equation can easily be solved numerically (fig 3). The solution consists in the intersection of a straight line and the sigmoid function. This intersection gives us the rest potential of the system with given parameters. Wanting that the intersection to be in the active part of the sigmoid, i.e. the part where the sigmoid values change significantly, one needs to impose $a_e > a_i$ and that's what we will assume in the rest of this project.

FIGURE 3 – Graphic solution for V_0

The solution is stable if $\frac{df}{dV}|_{V=V_0} < 0$, so the condition which ensures stability of the rest state is given as :

$$\left. \frac{dS}{dV} \right|_{V=V_0} < \frac{1}{a_e - a_i} \quad (15)$$

We then perform linear stability analysis with respect to space disturbances

$$V(x, t) = V_0 + \int dk u_k e^{ikx+\lambda(k)t} \quad (16)$$

with λ the growth rate and k the wave factor. This is injected in equation 11 while posing for simplicity $\alpha = 1$. Moving everything to the left-hand side, it appears that :

$$\lambda^2 + 2\lambda + 1 - \gamma \left[\frac{1 + \frac{\lambda}{v}}{k^2 + (1 + \frac{\lambda}{v})^2} a_e - \frac{r + \frac{\lambda}{v}}{k^2 + (r + \frac{\lambda}{v})^2} r a_i \right] = 0 \quad (17)$$

where

$$\gamma = \left. \frac{dS}{dV} \right|_{V=V_0} \quad (18)$$

We will use this parameter as control parameter as it has unique dependence (see 3) with P_0 instead of P_0 directly.

2.3.1 Turing patterns

Monotonic instability leads to stationary and inhomogeneous patterns (self-organized states). In the following lines, it will be the main focus of the analysis.

In this case, $\lambda = 0$ is used because the solution must be stationary so the growth rate is null.

If we take equation 17, rewrite to get the expression of a sixth order polynomial of λ . We then evaluate the expression of γ_c , the value of γ where λ changes sign :

$$\gamma_c(k) = \frac{r^2 + (1 + r^2)k^2 + k^4}{(a_e - a_i)r^2 + (a_e - a_i r^2)k^2} \quad (19)$$

One can remember the criteria of stability we established with equation 18. Taking this into account, to obtain (monotonic) instability, one must have $\gamma_c > \frac{1}{a_e - a_i}$

For the case of local excitation and lateral inhibition, ($r < 1$ according to plot 1), equation 19 can have a minimum smaller for some finite k (4). We can see on this plot that for $r > 1$, no such minimum exist and Turing patterns can't be formed. We can see that a minimum actually exist for $r^2 < \frac{a_e}{a_i}$, confirming $r < 1$. So in order to have Turing patterns formation, one must have the range of excitation smaller than inhibition. So Turing patterns require the neural field to excite locally and inhibit laterally. Notice that in this case, the speed of propagation v plays no role once the steady-state have been reached (see in the numerical resolution section).

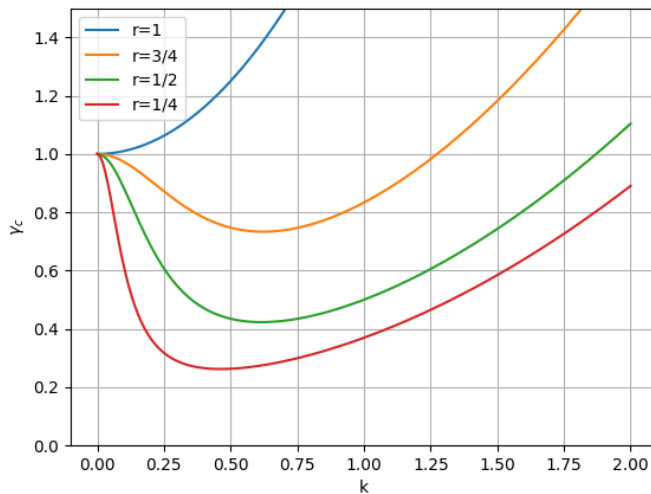


FIGURE 4 – Critical γ_c for Turing instability for several r

3 Numerical results

In this section, we aim to simulate the model modelling equation 11. This is a second order differential equation with respect to time. In order to solve it numerically, this assumptions is made $\partial_t V(x, t) = \Phi(x, t)$ and it is injected in 11 and everything is moved to the right-hand side, except the second order derivative which has become $\partial_t \Phi(x, t)$, and finally it results in the following system :

$$\partial_t V(x, t) = \Phi(x, t) \quad (20)$$

$$\partial_t \Phi(x, t) = -2\Phi(x, t) - V(x, t) + J(x, t) + \mu P(x, t) \quad (21)$$

The term $J(x, t)$ is actually the term that account for all non-linearities :

$$J(x, t) = \frac{1}{2} \int_{\Gamma} dx' (a_e e^{-(|x-x'|)} - a_i r e^{-(|x-x'|)r}) \times S\left[V(x', t - \frac{|x-x'|}{v})\right] \quad (22)$$

This $J(x, t)$ emphasizes 2 integrals of the shape :

$$I(x, t) = \int_{x-\frac{L}{2}}^{x+\frac{L}{2}} dx' F\left(x', t - \frac{|x-x'|}{v}\right) e^{-\eta(|x-x'|)} \quad (23)$$

$$= \int_0^L du (F(x-u, t - \frac{u}{v}) + F(x+u, t - \frac{u}{v})) e^{-\eta u} \quad (24)$$

To solve this integral numerically, a grid with $N+1$ mesh points separated from each other by the same distance $\Delta U = L/N$ is used. It gives :

$$I(x, t) = \int_0^L du G(x, u, t) e^{-\eta u} \quad (25)$$

$$= \sum_{n=0}^{N-2} \int_{u_n}^{u_{n+1}} du G(x, u, t) e^{-\eta u} \quad (26)$$

Please note that $u_n = n * \Delta u$. G is such defined as :

$$G(x, u, t) = (F(x - u, t - \frac{u}{v}) + F(x + u, t - \frac{u}{v})) \quad (27)$$

$$\approx G(x, u_n, t) + \frac{G(x, u_{n+1}, t) - G(x, u_n, t)}{\Delta u} (u - u_n) \quad u_n \leq u \leq u_{n+1} \quad (28)$$

because the G function varies little between two mesh point, so a linear approximation that makes little error is made. Inserting this last result in 26, the equation of I is given as :

$$I(x, t) \approx \frac{1}{\eta^2 \Delta u} \sum_{n=0}^{N-1} e^{-\eta u_{n+1}} \left[G(x, u_{n+2}, t) - 2G(x, u_{n+1}, t) + G(x, u_n, t) \right] \quad (29)$$

$$+ \frac{1}{\eta} \left[G(x, 0, t) + \frac{G(x, \Delta u, t) - G(x, 0, t)}{\eta \Delta u} \right] \quad (30)$$

$$- \frac{1}{\eta} e^{-\eta L} \left[G(x, L, t) + \frac{G(x, L, t) - G(x, L - \Delta u, t)}{\eta \Delta u} \right] \quad (31)$$

where the last term, often noted k is a correction term coming from the fact the length is finite.

For practical considerations to solve the system, the space L will be periodic, meaning that when we overlap one of the boundaries, we cross the other one. In practice, an overlap can occur when :

- $x - u < 0$, in this case, N is added to $x - u$
- $x + u > N + 1$, in this case, N is subtracted to $x + u$
- $t - \frac{u}{v}$, in this case, the function G is equal to twice the value of F evaluated before the perturbation so $G=2*F(V_0)$.

To compute V and Φ , an iterative method is used and it consists uses a forward Euler integration scheme is used. Using this scheme, Eq. 20 and 21 can be written as follows :

$$\begin{aligned} \partial_t V(x, t) &= \frac{V(x, t+1) - V(x, t)}{\Delta t} = \Phi(x, t) \\ \partial_t \Phi(x, t) &= \frac{\Phi(x, t+1) - \Phi(x, t)}{\Delta t} = -2\Phi(x, t) - V(x, t) + J(x, t) + \mu P(x, t). \end{aligned}$$

It leads to :

$$V(x, t+1) = \Phi(x, t) * \Delta t + V(x, t)$$

$$\Phi(x, t+1) = (-2\Phi(x, t) - V(x, t) + J(x, t) + \mu P(x, t)) * \Delta t + \Phi(x, t).$$

The system below can thus be computed in Python.

Finally, to have only adimension variables, we use α_1 and α_2 and r_e which means that $L_{dimensionless} = \frac{L[m]}{r_e[m]}$ and $v_{dimensionless} = \frac{v[m/s]}{r_e[m]\sqrt{\alpha_1\alpha_2[1/s^2]}}$.

4 Applications of the model

4.1 Turing patterns

From the section 2.3.1, a transient behavior leading to a stationary spatially periodic pattern is expected. Various parameters can be fixed as the following default parameters given in the Tab. 1. It is also important to notice that with the following parameter values, the regime is expected to be spatially periodic excitation pattern at its stationary state due to the fact that $r^2 < \frac{\alpha_i}{\alpha_e} \Leftrightarrow r < 1$.

Parameter	Value	Unit
L	0.05	m
N	400	-
a_e	6	-
a_i	5	-
α_i	400	s^{-1}
α_e	400	s^{-1}
μP	2.5	-
Δt	0.05	s
v	0.08	m/s
r_e	0.0005	m
r_i	0.001	m

TABLE 1 – Parameter values

The simulation for a random perturbation of magnitude $10^{-3} \times V_0$ for all of these parameters is represented on figure 5. V_0 is the potential at rest state obtained by solving the Eq. 15. By doing this, before the random perturbation (for $t < 0$), the voltage at all mesh point is equal to V_0 .

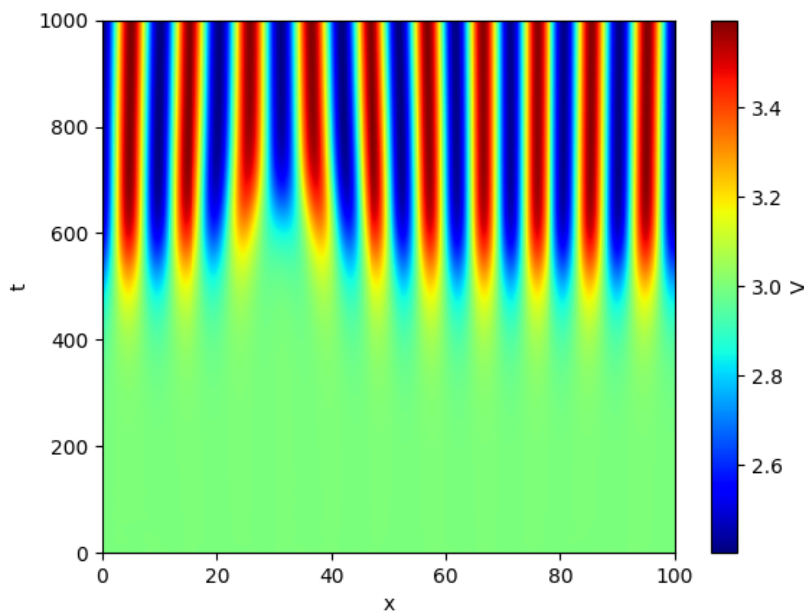


FIGURE 5 – Turing patterns with the default parameters

We can indeed observe a transient state and a periodic in space stationary behavior for $t > 700$, i.e. $t > 700 \times 0.0025 = 1,75s$. For $t < 400$, it appears that the membrane potential stay close to $3V$ which corresponds to the potential before the perturbation. The time needed to see a convergence of the model is not equal to the time needed to have Turing pattern in the article [Pattern formation in intracortical neuronal fields](#) but this difference can be explained by the fact that the perturbation at time 0 is not the same in our simulation than in the simulation's article. But, it leads to the same result. According to this, it shows that the effect of a perturbation on the potential is not immediate. As said before, Turing patterns are linked to monotonic instability which leads to stationary and inhomogeneous patterns. This behavior is shown on Fig. 5 and 6. Indeed, V takes periodic value in space which oscillate between 2.4 and 3.6. This behavior can be explained biologically by the fact that $r < 1 \Leftrightarrow \frac{r_e}{r_i} < 1 \Leftrightarrow r_e < r_i$. This inequality means that the inhibitory spread is less wide than the excitatory spread. Regarding that, it seems logical that dark red regions having a high potential correspond to excitatory field while the dark blue region having a low potential correspond to inhibitory field.

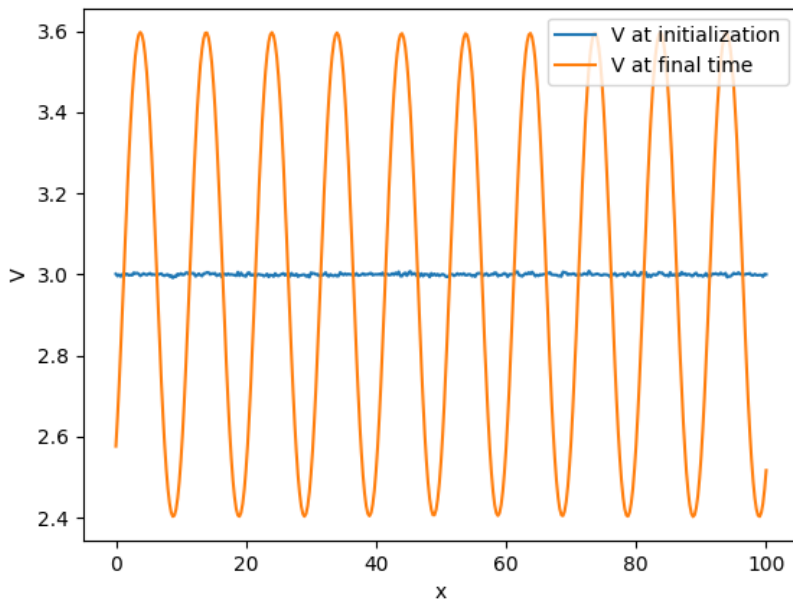
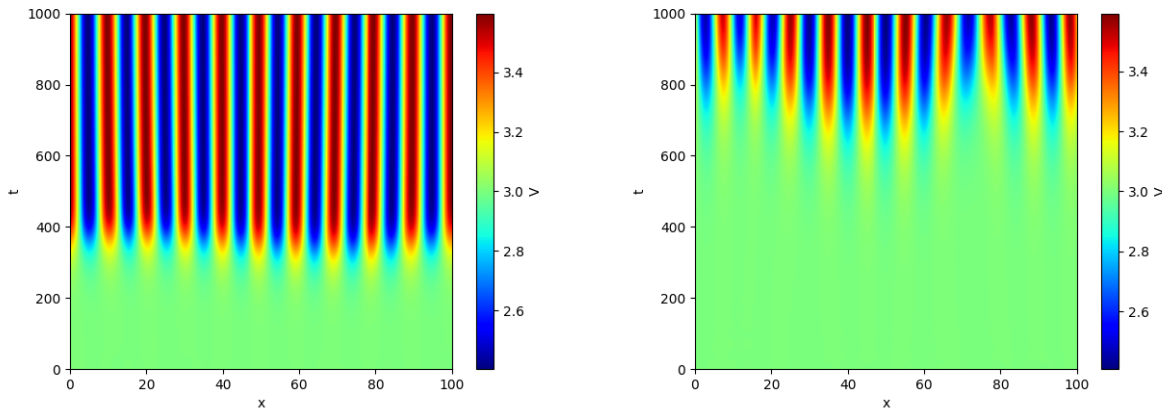


FIGURE 6 – Periodization in space representation

After this short analyze of Turing patterns, it can also be interesting to discuss a little bit about the changes caused by modifications of parameters.

4.1.1 Effect in changes of speed

First, the effect of the speed can be analyzed. The speed is modeled by the parameter v and is equal to $0.08m/s$ in the section. The only use of v in the model is in Eq. 23 to compute the delay. So, we can expect that an increase (resp. a decrease) of the value of the speed leads to a decrease (resp. an increase) of the delay and a shorter (resp. longer) time for the model to converge because values of V are less (resp. more) influenced by further values of the potential in time. In addition, a speed change should not affect the Turing patterns.



(a) Turing patterns with the default parameters but with $v = 0.16m/s$
(b) Turing patterns with the default parameters but with $v = 0.04m/s$

FIGURE 7 – Turing patterns with the default parameters but with variable v

Regarding the Fig. 7, our previous statement is confirmed because the speed doesn't influence the steady state patterns. Indeed, the only change in comparison with figure 5 is that the transient state is the only phase which is affected by this change of speed.

4.1.2 Effect of r_e and r_i

Secondly, it is possible to change r_e and r_i which are respectively the excitatory and inhibitory spread. To make this analyze, r_e and r_i will be multiplied by the same number to remain the ratio between these value r constant. The fact that r remains constant enables to keep a value of r smaller than one to garanty the appearance of Turin patterns. After this change, one should not expect big changes in the behaviour of the system because the only use of r_e or r_i is to adimensionalize L and v. So, an increase of r_e links to a decrease of the value of the adimensionalized length L and the speed v .

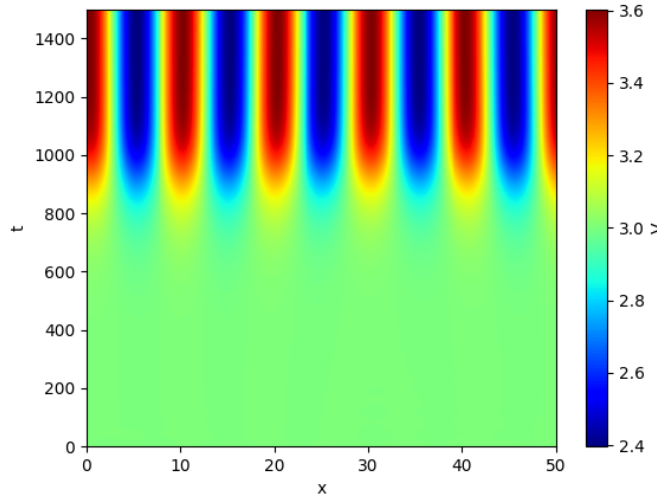


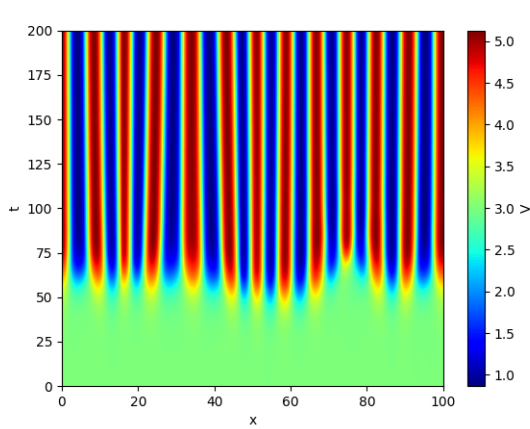
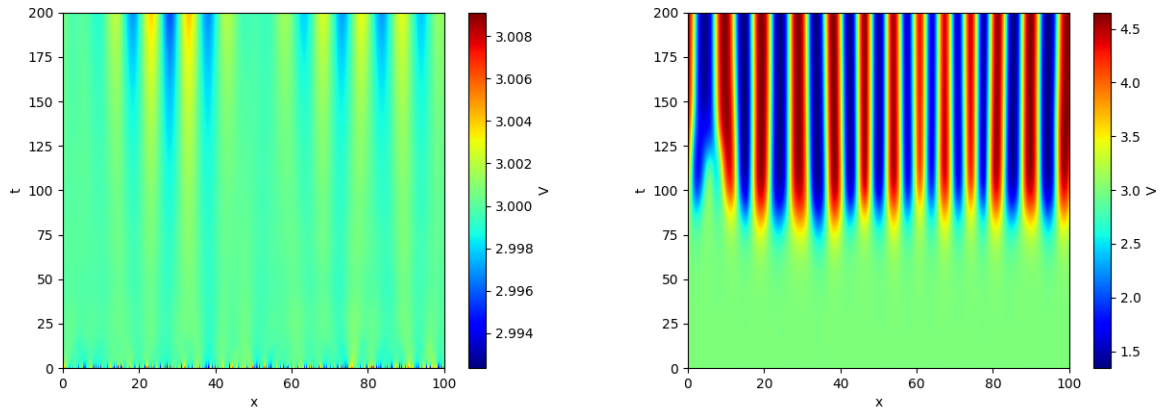
FIGURE 8 – Turing patterns with the default parameters but with $r_e = 0.0005 * 2$ and $r_i = 0.001 * 2$

Regarding Fig. 5 and 8, it validates the intuition explained earlier in this subsection. Indeed, the length L has decreased in the Fig according to an increase of the spread, it has been divided by two since both r_e and r_i are multiplied by 2. On the Fig. 8, the impression that the areas of inhibition and excitation are larger than those on the Fig. 5 but it remains to same. So, Turing patterns remain again there. In addition, it can also be seen that the Turing patterns appear later than for the basic plot due to the reduction of the speed v .

4.1.3 Effect of the parameter a_e and a_i

Thirdly, it is possible to modify the excitation a_e and the inhibition a_i . While doing this, it is important to remember that our model was build with the statement that $a_e > a_i$ so this inequality have to be respected.

After few simulations, it appears that a modification of one of the two parameters causes the disappearance of Turing patterns so the difference between a_e and a_i is kept equal. By doing this, it enables to have an initial potential equal to 3 regarding the equation 14.



(c) Turing patterns with the default parameters but with $a_e = 11$ and $a_i = 11$

FIGURE 9 – Turing patterns with the default parameters but with variable a_e and a_i

Regarding Fig. 9, it appears that increasing the value of a_e and a_i leads to a large reduced of the convergence time for Turing patterns. Another important thing to notice is that the

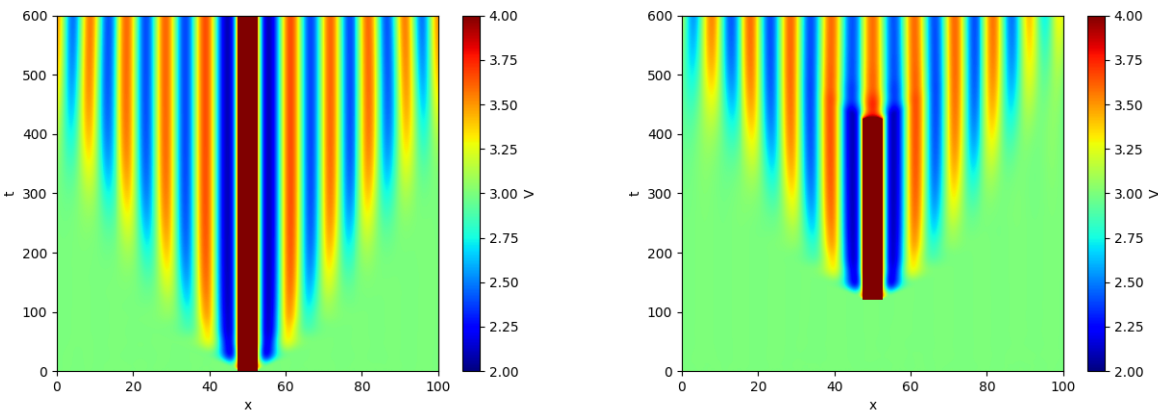
range of the values of the potential increases while a_e and a_i increase. It happens because the only appearance of these two parameters in the model is in the expression of $J(x, t)$ (and in the Eq. 14 but keeping the difference between a_e and a_i constant enables to get ride of this). It means that increasing the excitation and the inhibition leads to a slight increase of the absolute value of $J(x, t)$ which lead to an increase of $V(x, t + 1)$. Finally, a modification of a_e and a_i does not result in the disappearance of Turing patterns but just a change of the amplitude of the values taking by the potential.

4.1.4 Adding a local perturbation of the external pulse

In this subsection, the effect of the external perturbation on Turing patterns can be analyzed. After trying to modify the value of the external perturbation μP_0 , it appears that the Turing patterns disappear which is due to the fact that the initial condition derived from Eq. 14 is modified. To avoid this problem, the value of μP_0 is kept constant in order to have a potential before the perturbation equal to 3. It means that the only effect of a modification of external perturbation is applied on Eq. 21 for $\mu P(x, t)$. It is expected that an increase of $\mu P(x, t)$ leads to an increase of the derivation of Φ . To make a simulation, the external perturbation will be given by :

$$\mu P(x, t) = \begin{cases} \mu P_0 + Q(t) & \text{if } 0.475L \leq x \leq 0.525L \\ \mu P_0 & \text{otherwise} \end{cases}$$

with $Q(t)$ equal to 20.



(a) Turing patterns with the default parameters and (b) Turing patterns with the default parameters and local time-dependant perturbation

FIGURE 10 – Turing patterns with the default parameters and local perturbation

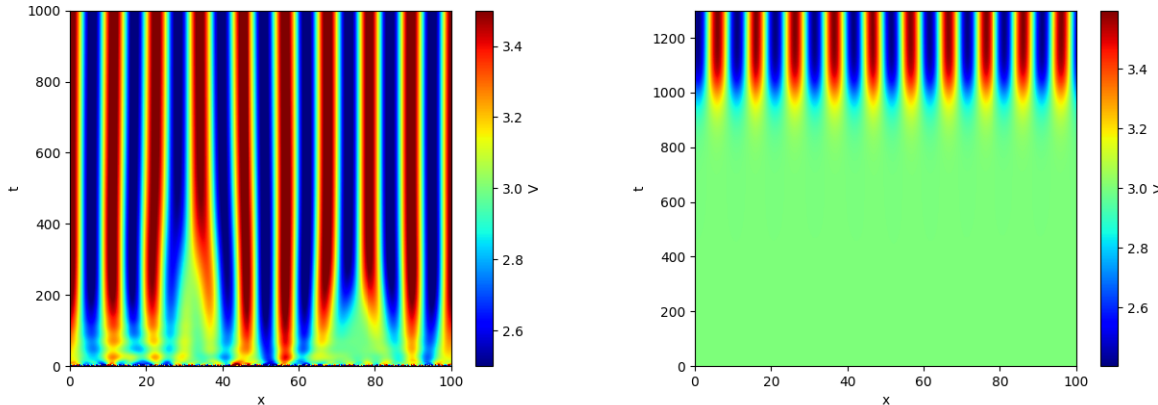
According to the discussion below, it appears on Fig. 10 that adding a local perturbation globally enables to have a shorter time of convergence. Indeed, compared to Fig. 5, it appears that Turing patterns appear when $t > 450$ for a local perturbation applied for every time and when $t > 550$ for a local time-dependant perturbation. It is also important to note that the closest points of the local perturbation are impacted at the beginning while the furthest points will be impacted later. This result can be explain by the fact that the model is an iterative one meaning that the next value of potential rely on the "old" value of potential through the adding of a little value. With a local perturbation, this little value incremented become larger meaning that it leads to have faster the convergence of the model. But, this higher incrementation is

just active for a little range of spatial value which explains that the closer a point is to the disturbance, the faster it will be returned to a zone of inhibition or excitation due to the limit speed of the propagation. Indeed, the value of $J(x,t)$ depends on the potential of the neighbors of the evaluated point. Knowing that the closer the neighbors are, the faster they will have an impact, so it seems logical that the perturbation needs time to impact all points.

After this analyze, it appears that a modification of μP_0 leads to no Turing patterns while a local modification of $\mu P(x,t)$ leads to a fastest convergence of the model to Turing patterns.

4.1.5 Modification of the initial condition

To make the Fig. 5, a normal perturbation with a standard deviation equal to 10^{-3} in the initial condition is applied on the initial potential. By doing this, it leads to the apparition of Turing pattern when t is higher than 600. In this subsection, the amplitude of the variance is changed. Indeed, it can be seen on Fig. 11(a) that an increasing of the amplitude of the initial perturbation enables to the model to converge faster. In this case, when t is higher than 400, Turing patterns can fully be seen. On the other hand, when the amplitude of the initial perturbation of the potential decreases, the model converges slower which leads to the apparition of Turing patterns when t is higher than 1100. It can be explained by the fact that this model is an iterative one. So, by applying an higher perturbation of potential at the initial potential, the model will be closer to the threshold and the difference between two iterations will be higher which enables the Turing patterns to appear faster. It is also good to notice that the amplitude of the excitatory and the inhibitory areas does not change.



(a) Turing patterns with the default parameters and (b) Turing patterns with the default parameters and initial condition of amplitude equal to 10^{-6}

FIGURE 11 – Turing patterns with the default parameters with different initial conditions

4.2 Waves

In this section, the regime which will be investigated is an oscillatory regime. To do so, the excitatory spread will be greater than the inhibitory spread meaning that $r_e > r_i$. By doing this, the creation of Turing pattern is prevented and it is a case of local inhibition and lateral excitation. To fully investigate all the possible regime and avoid to be in a stable regime, it can be interesting to remember the Fig. 12 from the article. Regarding this figure, it appears the parameter r cannot be too small in order to have an oscillatory regime.

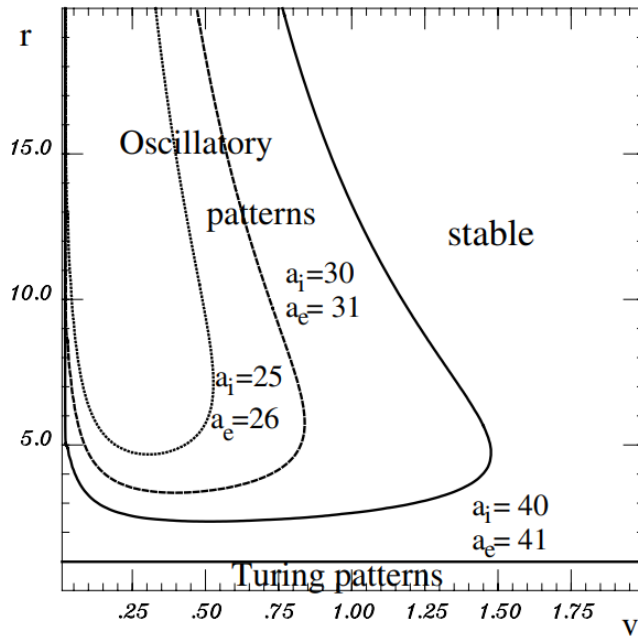


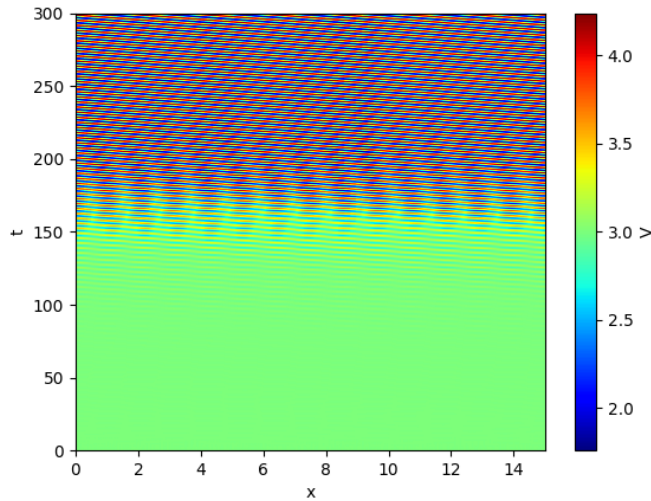
FIGURE 12 – Phase diagram of instabilities

4.2.1 Homogeneous external stimulation

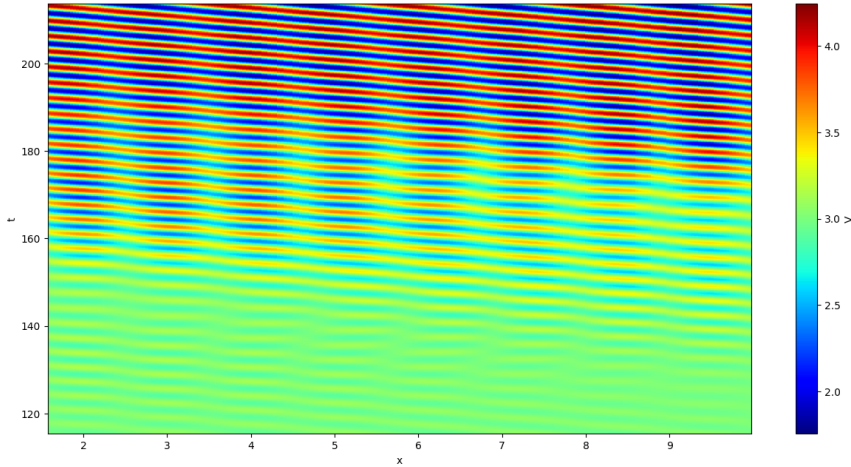
First, oscillatory regime with a homogeneous external stimulation will be investigated meaning that μP_0 is kept constant. To make simulation, the various parameters are set to values in the Tab. 2. With this value of r_e and r_i , the parameter r is equal to 2, 7 which is quite low and very close to the instability shown in the Fig. 12.

Parameter	Value	Unit
L	0.015	m
N	400	-
a_e	41	-
a_i	40	-
α_i	400	s^{-1}
α_e	400	s^{-1}
μP	2.5	-
Δt	0.05	s
v	0.3	m/s
r_e	0.00037	m
r_i	0.001	m

TABLE 2 – Parameter values



(a) Homogeneous external stimulation close to the instability



(b) Zoom on standing waves

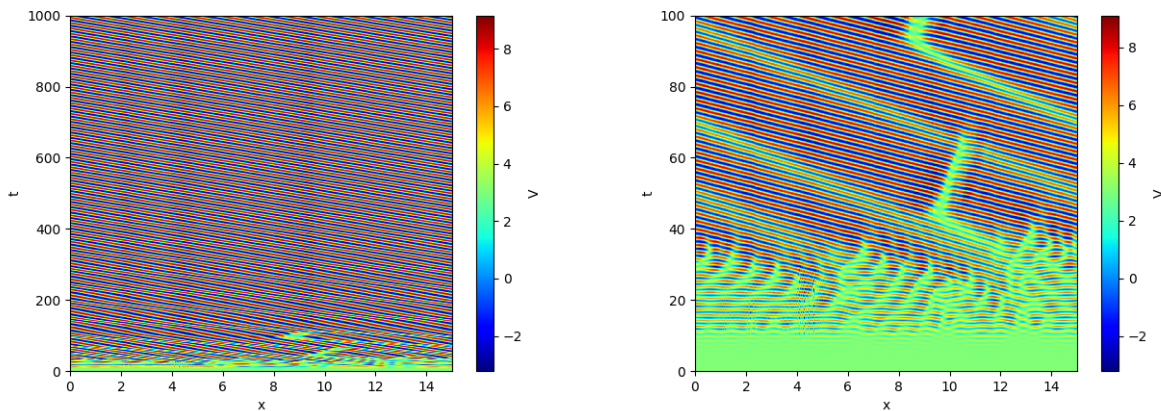
FIGURE 13 – Homogeneous external stimulation close to the instability

It appears on Fig. 13 that an oscillatory state takes place at time 200 which corresponds to 0.5s in physical time. In that case, oblique bands corresponding to relatively regular travelling waves crossing the calculation domain can be observed. It is the oscillatory regime which is expected. Another important thing is to note that there is a transient state between the perturbation and the effect of it. It is interesting to notice that this transient time is smaller in that case than in the previous section which is logical according to the increase of the speed. During this transient time, two behaviors can be highlighted. First, the potential stays close to the initial potential and when t is greater than 150, standing waves can be seen on Fig. 13(b)

To have a clear vision of the oscillation regime, a simulation with a large value of parameter r can be done to see how the model reacts away from the instability. According to this requirement, the parameter values are given in the Tab. 3 and the parameter r is equal to 10.

Parameter	Value	Unit
L	0.015	m
N	400	-
a_e	101	-
a_i	100	-
α_i	400	s^{-1}
α_e	400	s^{-1}
μP	2.5	-
Δt	0.05	s
v	0.3	m/s
r_e	0.001	m
r_i	0.0001	m

TABLE 3 – Parameter values



(a) Homogeneous external stimulation away from the instability
 (b) Zoom on homogeneous external stimulation away from the instability

FIGURE 14 – Homogeneous external stimulation away from the instability

On the Fig. 14, the behavior of the potential is shown for a regime far away from the instability. In this case, some differences are presented compared to the previous case where the regime was close to the instability. Compared to Fig. 13, travelling waves appear very quickly. In the beginning, standing waves does not have the same wavelength but it stays in the same range of value. When t is greater than 40, the wavelength stays the same but there are localized defects between the travelling waves. These localized defects moves with a lower speed than the waves speed. The speed of a travelling wave and the defect can be seen using the Fig. 14(b). To do so, the slope of a wave is measured and represents the speed. Visually, it appears that defects need more time to spread. It enables to system to have the property of memory so it acts like a dynamic system. According to the observation of the article, the defects moves in the opposite direction of the travelling waves.

4.2.2 Inhomogeneous external stimulation

In the previous subsection, travelling waves and defects have been shown which links to a system with memory. A good question now can be : "How to erase this information which

is stored ?". On the article, an idea of solution is to impose an external localized stimulus. It means that the external potential is not kept constant this time and can be defined as :

$$\mu P(x, t) = \begin{cases} \mu P_0 + Q(t) & \text{if } 0.475L \leq x \leq 0.525L \\ \mu P_0 & \text{otherwise} \end{cases}$$

with $Q(t)$ equal to 20.

First, to see the impact of an added inhomogeneous external stimulation and to compare the result with Fig. 13, the values of the various parameters are set to the values in the Tab. 2 except for which can vary as 4.2.2. In that case, $Q(t)$ does not depend on the time so the perturbation is added for every value of time but only for a certain range of spatial value.

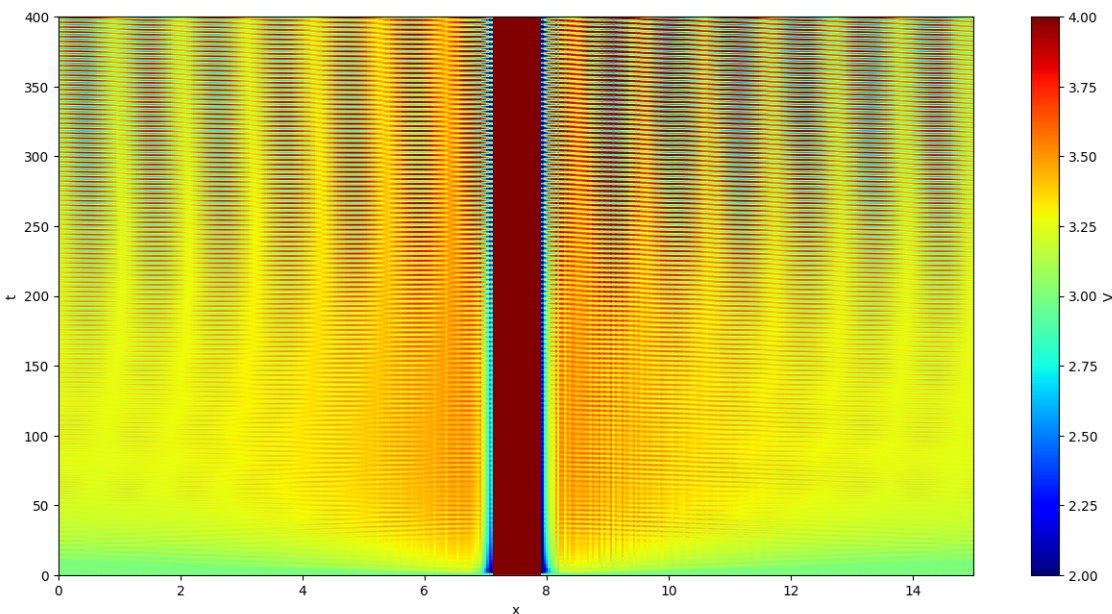


FIGURE 15 – Inhomogeneous external stimulation

After the simulation, the Fig. 13 and the Fig. 15 can be compared. In these two cases, the value of the parameters leads to the creation of waves which means that the regime is an oscillatory regime which seems logical. It means that the value of the external perturbation does not change the regime of the system. It is also important to notice that the waves are not the same for these two figures. In the basic case, there are standing waves at the beginning which become travelling waves. In the inhomogeneous case, there are just travelling waves due to the apparition of the local perturbation. It means that a local perturbation can change the behaviour of the system.

Secondly, to understand the effect of a local perturbation on the system which has the property of memory, the values of the parameters of the Tab. 3. In that case, $Q(t)$ depends on the time and is added for certain time.

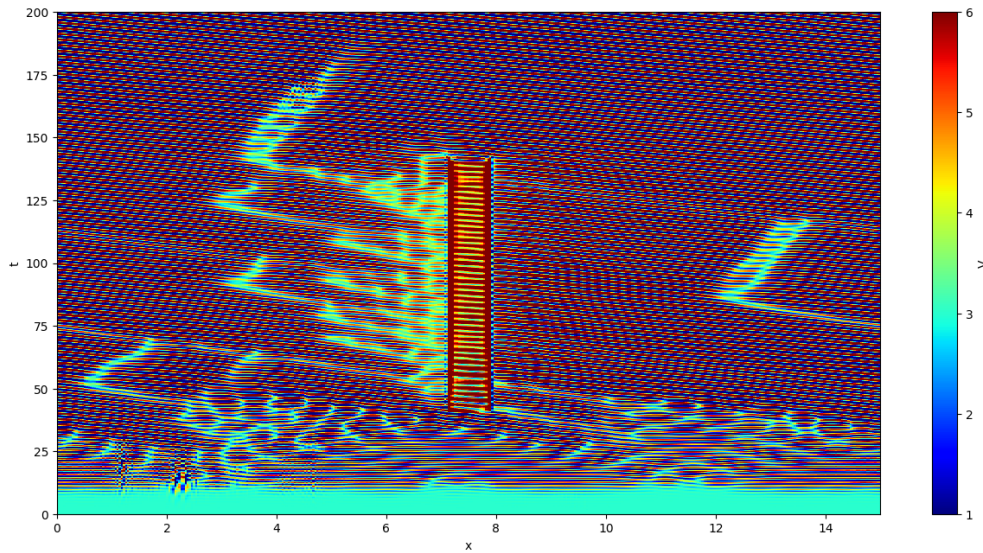


FIGURE 16 – Oscillatory regime away from the instability

As expected, defects can be seen on Fig. 16 due to the fact that the ratio of spatial scale r is equal to 10 so it is far away from the instability. Regarding Fig. 14, it appears that waves are present in the two cases. It means that away to the instability, the regime and also the global behaviour of the system remains the same. The big difference between this two figures is that the local perturbation erases the defects. this can be seen on the right of the perturbation where a defect begins to appear and due to the local perturbation, this defect is erased. This does not happen immediately due to the limited speed.

5 Conclusion

The study enables us to account for excitatory and inhibitory contributions in a neural field having the spatial and temporal effect.

Thanks to this model, it enables us to test the parameter combinations that lead to the different types of instability. To have Turing patterns, it is necessary to have a local excitation and a lateral inhibition. A change of speed or the parameters r_e and r_i with $r < 1$ or the parameters a_i and a_e with a difference between them equal to one or the local perturbation leads to the appearance of Turing patterns. It seems logical according to the fact that the Turing patterns are caused by intrinsic properties and not by an external constrain. On the other hands, oscillatory instability can occur with local inhibition and lateral excitation. In this case, the type of waves can change according to the distance of the instability and to the adding of a local perturbation but waves remain here in all cases.

Finally, the numerical simulations confirm the results of the reference article. This model can therefore be used to model the behavior of our neural system when subjected to different situations. In order to be applicable and to be a perfect representation of reality, a more complex and less restrictive model can be searched.